

Investigation on PEEK Fabrication Using Mask-image-projection-based Stereolithography

Dongping Deng, Yong Chen*, Chi Zhou

Epstein Department of Industrial and Systems Engineering
University of Southern California, Los Angeles, CA 90089

*Corresponding author: yongchen@usc.edu, (213) 740-7829

Abstract

This paper presents the findings of an initial study of the fabrication of polyetheretherketone (PEEK) components based on the mask-image-projection-based Stereolithography (MIP-SL) process. PEEK is a semicrystalline thermoplastic with excellent mechanical and chemical resistance properties that are retained to high temperatures. It has been extensively used in the aerospace, automotive, biomedical, and chemical process industries. The fabrication process based on the MIP-SL includes both green-part fabrication and the sintering of fabricated green parts. In the green part fabrication, the challenges of recoating viscous composite slurry are discussed. A prototype system has been developed for the fabrication of green-parts with complex shapes and small features. Based on the fabricated green-parts, the challenges in the sintering process for achieving desired functionality are discussed. The test results on the sintered PEEK components have also been presented. Future work based on the study has been identified.

Keywords: PEEK composite, mask projection stereolithography, slurry recoating, sintering.

1. Introduction

Polyetheretherketone (PEEK) plastic is a high performance polymer with good mechanical, chemical, electrical and thermal properties. Its extraordinary properties including strength, stiffness, wear resistance, and high service temperature make it widely used in various industries [1-4]. In addition, because PEEK is a very stable material, it is often used as the matrix for other embedded materials such as carbon fiber or nano particles in order to get composite materials that have specific properties [5, 6]. Traditionally, the fabrication process of PEEK components is molding and hot pressing, in which the PEEK powder as well as other additive particles is filled in a mold with raised temperature and high pressure [7]. However, the fabrication methods only enable PEEK parts with relatively simple shapes. For fabricating parts with more complex shapes, problems such as the high cost of molds and long production process exist.

With the development of Additive Manufacture (AM) process, the manufacturing of PEEK parts with complex shape has been studied based on the Selective Laser Sintering (SLS) process [8, 9]. The method is at the early stage with more work to be done on the melting and crystallization as well as the kinetics and time-temperature behavior of the process. Motivated by the importance of PEEK components in future engineering applications, we investigated the use of another AM process in the fabrication of PEEK components.

The mask-image-projection based Stereolithography (MIP-SL) is an AM process, in which projection images are projected on photosensitive resin. An illustration of the MIP-SL process is shown in Figure 1a. The mask images can be dynamically defined by a Digital Micromirror Device (DMD) [10, 11] with micro mirrors that can turn on or off a pixel. In the MIP-SL process, a 3-Dimensional (3D) model of a designed part is first sliced into layers of 2-Dimensional (2D) mask images. The mask images are then sent to a DMD and projected on a liquid resin surface. The photocurable resin is selectively cured and forms one layer. The fabrication of next layer goes on after raising the Z-stage. The building job of the designed part is finished until all the layers have been built.

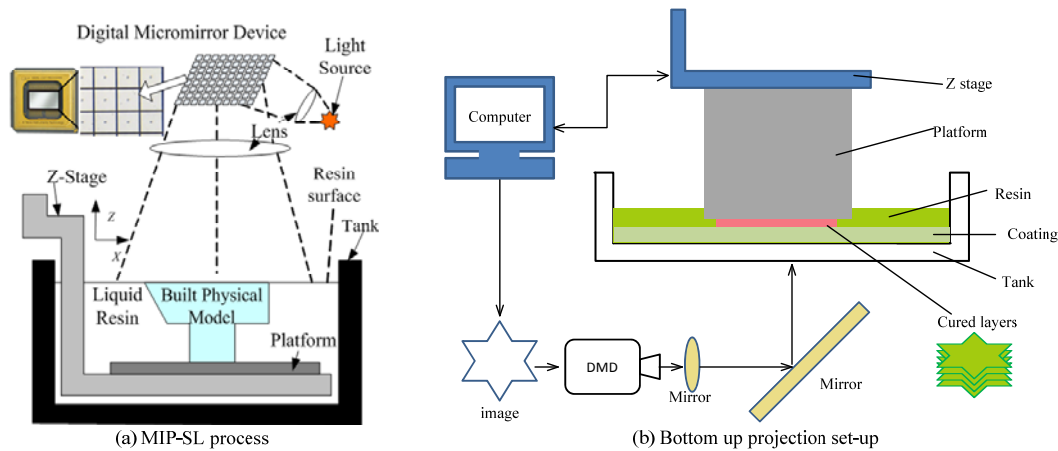


Figure 1. An illustration of the MIP-SL process and a bottom-up projection setup.

Figure 1b shows a bottom-up projection setup that can be used in the MIP-SL process. In the setup, the layer thickness of the part can be well controlled due to the constraint curing. However, the separation force between the tank and the cured layer could be large. Zhou, *et al.* [12] studied the separation force and presented a two channel tank for the bottom-up MIP-SL system. The developed two channel design is shown in Figure 2, in which half of the tank is coated with a PDMS film while the other half has no coating. The separation force between the cured layer and the tank becomes much smaller by moving the platform from the left channel (i.e. the channel with PDMS film coating) to the right channel (i.e. the channel without PDMS film coating) before lifting the platform up.

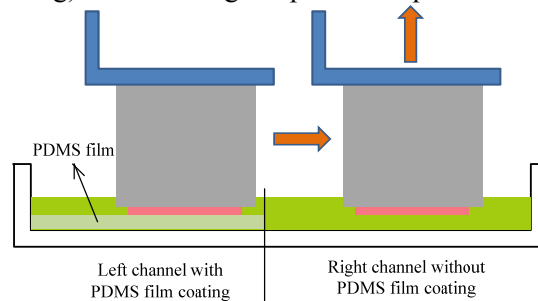


Figure 2. A two-channel tank design for the bottom-up projection setup.

In this paper, we investigated the two channel design for the fabrication of green parts of PEEK composite. We also studied the sintering process and material properties of sintered PEEK composite parts. The paper is organized as follows. An overview of the PEEK fabrication process is described in section 2. The green part fabrication based on the MIP-SL process is discussed in Section 3. The sintering process is presented in Section 4. Section 5 presents the testing results on various material properties of the fabricated parts. Finally we draw conclusions in Section 6.

2. Process Overview

Similar to the fabrication process of PZT components [13], our PEEK fabrication process includes two major steps, green part fabrication and sintering of the fabricated green parts. An illustration of the process is shown in Figure 3. In order to use the MIP-SL process, composite slurry is first produced by mixing PEEK powder and photosensitive resin. The PEEK slurry should be mixed well in order to fabricate good quality parts. After the slurry has been prepared, the green parts with desired shapes can be fabricated using the MIP-SL process. A main challenge in this step is the recoating of the PEEK slurry which can have a much higher viscosity due to the addition of PEEK powder. Finally, green parts are sintered for achieving improved material properties. The challenge in this step is to understand the proper settings of the sintering process such that the fabricated PEEK parts can have desired material properties.

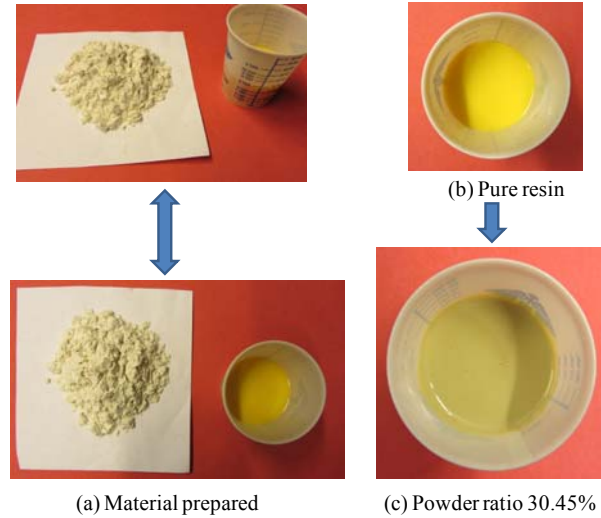
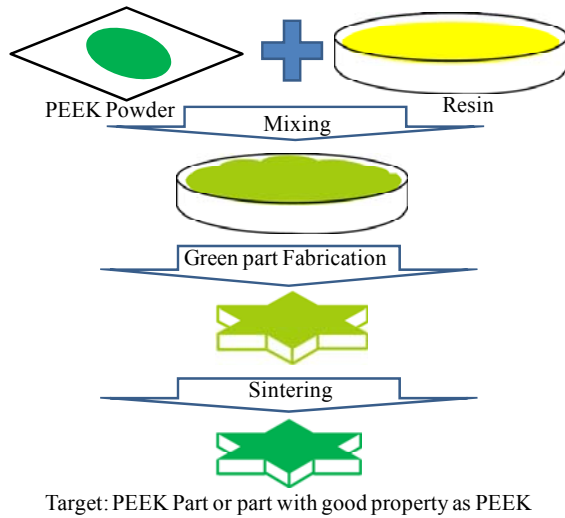


Figure 3. An illustration of the developed AM process.

Figure 4. The procedure of preparing slurry.

The preparing of PEEK slurry is important. It is desired to have homogenous slurry such that the fabricated parts could have isotropic property. The PEEK powder used in our study is PEEK 150PF from VICTREX Co. The powder is in spherical shape with particle size of 40 μm . The photocurable liquid resin used in our study is SI500 from EnvisionTec Inc. A precision weight scale was used in determining the weight ratios of the PEEK slurry and a stirring machine was used in preparing the slurry. An example of the PEEK slurry is shown in Figure 4.

The viscosity of the mixed slurry increases with a higher weight ratio of PEEK powder in the mixture. When more powder is added, the mixed slurry will have a higher viscosity. Accordingly we can classify the PEEK slurry into three groups.

- (1) **Slurry that can flow:** When the ratio of the PEEK powder in the slurry is less than 27.5%, it is observed that the slurry can flow to refill voids during the recoating process;
- (2) **Slurry that cannot flow but can attach to dipped surfaces when taking out:** When the ratio of the PEEK powder in the slurry is between 27.5% and 33.8%, it is observed that the slurry cannot flow by itself but can attached to surfaces that are dipped into the slurry;
- (3) **Slurry that cannot flow or attach to dipped surfaces:** When the ratio of the PEEK powder in the slurry is over 33.8%, the mixture is similar to paste. It cannot flow or be spread out easily. Further, it will not attach to dipped surfaces.

In our study, we also found that the stirring of the mixture becomes rather difficult when the weight ratio of the PEEK powder is above 37%. It is possible to reduce the slurry's viscosity by adding chemical solutions such as isopropanol; however, the material properties of the fabricated PEEK parts may also be affected by the additional solutions. We only tested the PEEK slurry by directly mixing PEEK powder with liquid resin in our study. A better slurry preparation approach is desired for achieving a higher percentage of PEEK powder in the mixed slurry in the future research.

3. Green Part Fabrication

For each group of the slurry with different viscosities, we developed corresponding material refilling strategies in the bottom-up MIP-SL process.

3.1 Fabricating green parts with slurry that can flow

For the slurry in the first group, we used the two channel system that was developed for liquid resin. Since the slurry can flow by itself, the fabrication procedure in building green parts is similar to the one as presented in [12], which is shown in Figure 5.

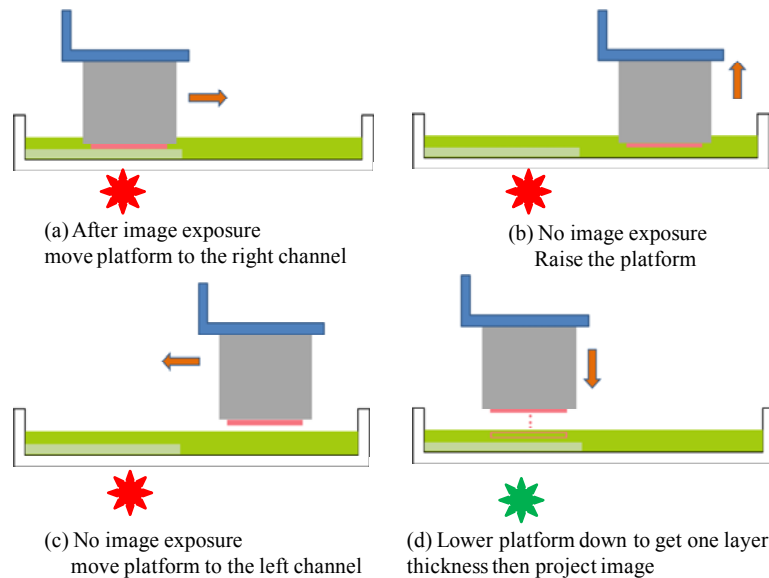


Figure 5. Green part fabrication for the first group of PEEK slurry.

3.2 Fabricating green parts with slurry that can attach to dipped surfaces

For the slurry in the second group, the slurry cannot flow freely on the PDMS surface; however, it can attach to dipped surfaces. We used a modified fabrication procedure as shown in Figure 6. After the build part and the platform are moved rightward to the channel without the PDMS film (Step b). We move them down by a certain distance d and dip into the slurry (step c). The attached slurry on both bottom and side surfaces can bring certain amount of material that is adequate for building a new layer. Although the amount of the material attached to the dipped surfaces requires more effort to model, it is observed that more materials will be brought up if the distance d is larger. In addition, it was found that the dipped material cannot be evenly spread out on the PDMS film when the platform was lowered to form one layer thickness (step f). In order to fill the whole gap related to the next layer with slurry, an addition “rubbing” mechanism is used in our fabrication procedure. As shown in step g and h, the part is moved left and right to better spread the dipped material on the PDMS film.

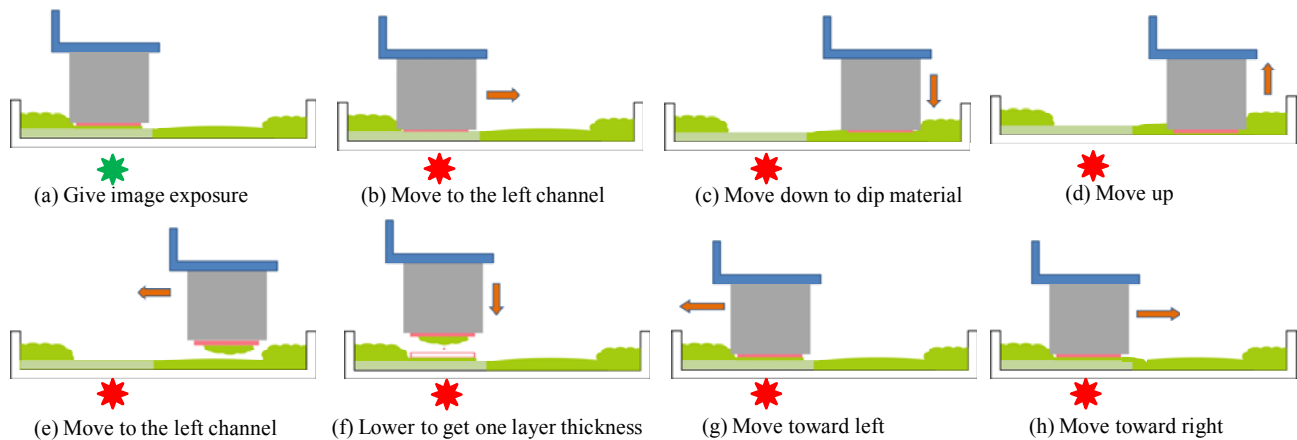


Figure 6. Green part fabrication for the second group of PEEK slurry.

Figure 7 shows a part that was built with and without extra rubbing motion. For a layer with a big area, the lack of material will cause defects in the cured layer. Note that a previous layer that was incompletely built will adversely affect all the following layers. The advantage of using “rubbing” mechanism is that the material can be spread out evenly; however, a drawback is that small features on the part could be broken during the “rubbing” movement.

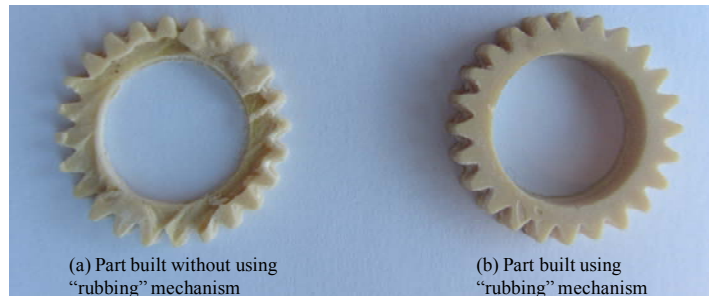


Figure 7. A comparison of built parts with and without the “rubbing” mechanism.

3.3 Fabricating green parts with slurry that cannot flow or attach to dipped surfaces

For the slurry in the third group, it cannot flow freely nor attach to dipped surfaces. Instead, additional spreading forces are required that can push the slurry into the formed gap related to a new layer. In our experiments, we used a simple design as shown in Figure 8a for “pushing” the paste-like slurry. In the design, we fill slurry in a closed tank that contains the platform inside. As shown in Figure 8b, the slurry will be pushed to fill the region related to the next layer when the platform is moved back and force.

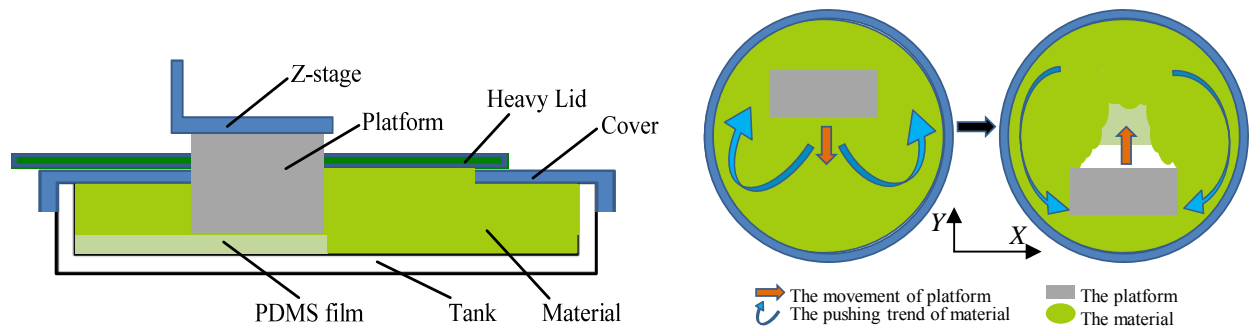


Figure 8. The design of the “pushing” mechanism.

Accordingly, a modified fabrication procedure is shown in Figure 9. As shown in the illustration, the slurry in the enclosed tank is pushed between the left and right channels when the platform is moved. Consequently, the slurry can be ensured to refill the left channel when the platform is moved down to form a new layer. Note that there will be certain void generated in the tank during the building process. This is because the platform is moved upward by a layer distance while the total volume of the tank is fixed. To refill the void, additional slurry can be estimated and added into the tank during the building process.

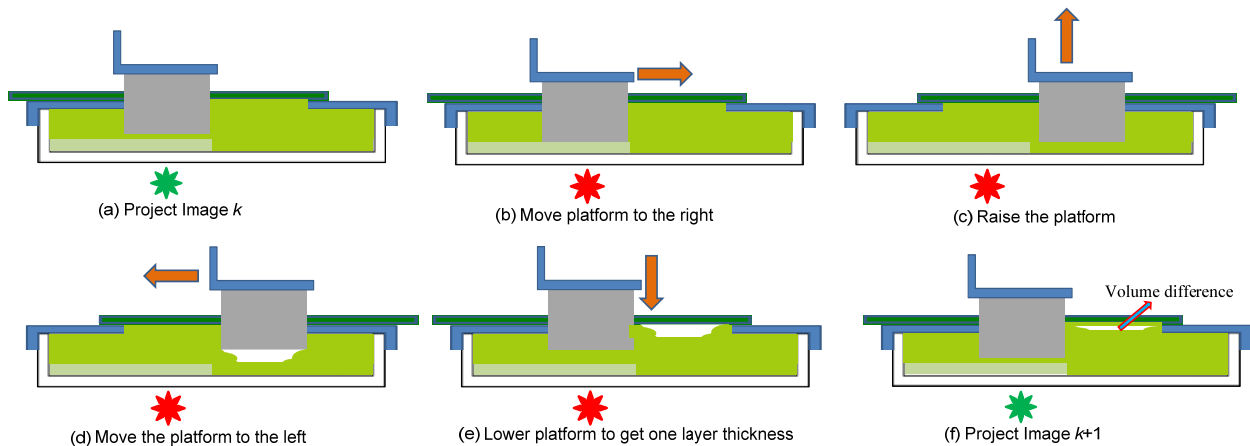


Figure 9. Green part fabrication for the third group of PEEK slurry.

Figure 10 shows the building results of some test parts based on the developed “pushing” mechanism. As shown in the testing results, the simple approach can ensure the uniform spreading of the slurry on the PDMS film for forming thin layers (50 μm used in the tests).

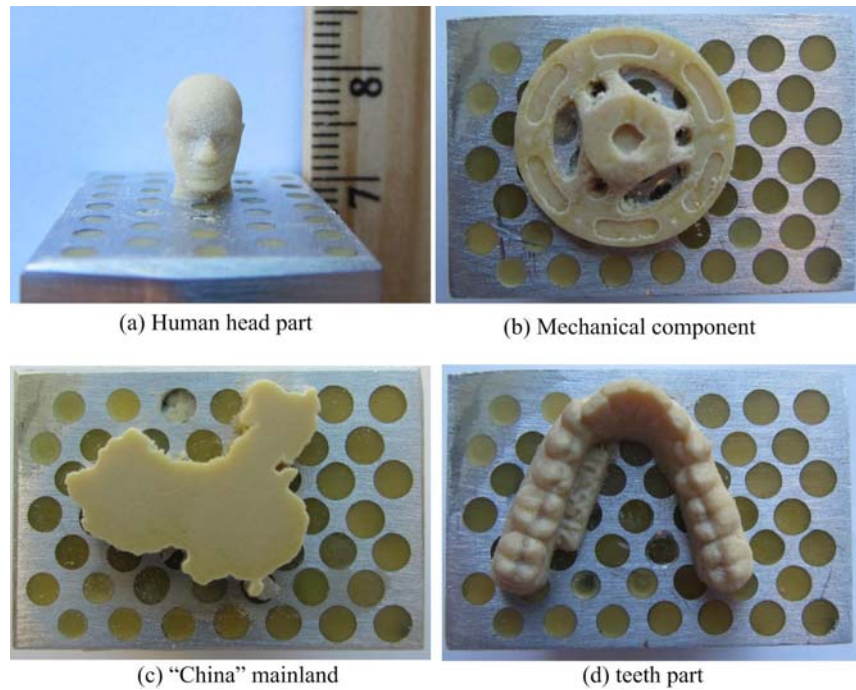


Figure 10. Built parts using the “pushing” mechanism for the third group of PEEK slurry.

3.4 Cleaning procedures of green parts

Comparing to the MIP-SL process for liquid resin, the cleaning procedure for PEEK slurry is relatively more difficult due to the higher viscosity value of the slurry. The procedures we used in our tests include following steps with an example as shown in Figure 11.

- (1) Remove the part from the platform and gently clean it with a soft paper napkin;
- (2) Clean the part using an ultrasound cleaner filled with isopropyl alcohol for 10 minutes;
- (3) Use an electric fan to dry the part and remove alcohol;
- (4) Use a brush to clean any residue attached to part surfaces.

Steps (2)-(4) may be repeated if the part has some hard-to-clean features such as deep holes.

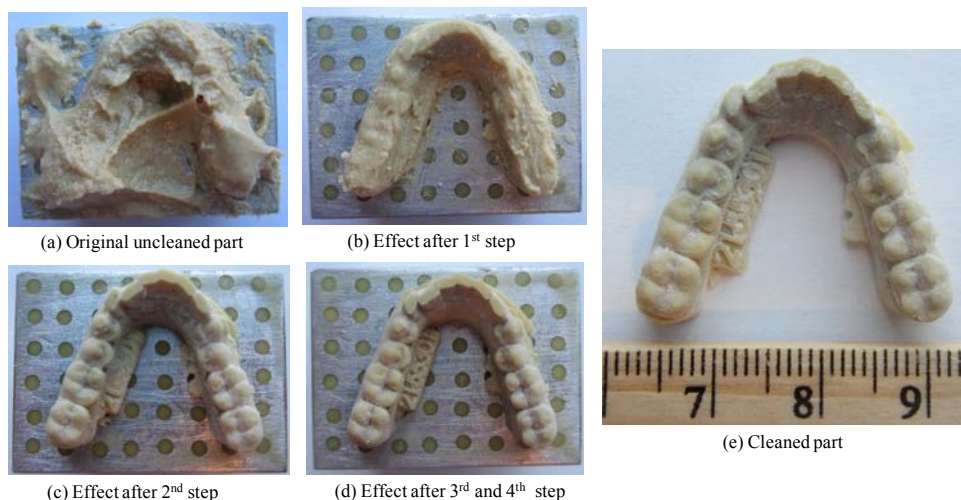


Figure 11. An illustration of the cleaning steps and related effects.

4. Sintering Process of Green Parts

The slurry-based MIP-SL process can build parts with the desired shapes defined by computer-aided design (CAD) models. In this paper, we call such parts without heat treatment “green parts”. Since the fabricated green parts may not have the desired material properties, we studied the sintering of green parts and related material property changes.

PEEK is a semicrystalline thermoplastic with the glass transition temperature of $\sim 143^{\circ}\text{C}$ and the melting point of $\sim 343^{\circ}\text{C}$. In comparison, the photopolymer used in our study (SI500) has a glass transition temperature of 61°C . Accordingly, the heat treatment procedure we designed is shown in Figure 12. Various sintering temperatures ranging from 200°C to 320°C were set on the temperature curve. During the sintering process, a furnace filled with nitrogen was used to avoid oxidation.

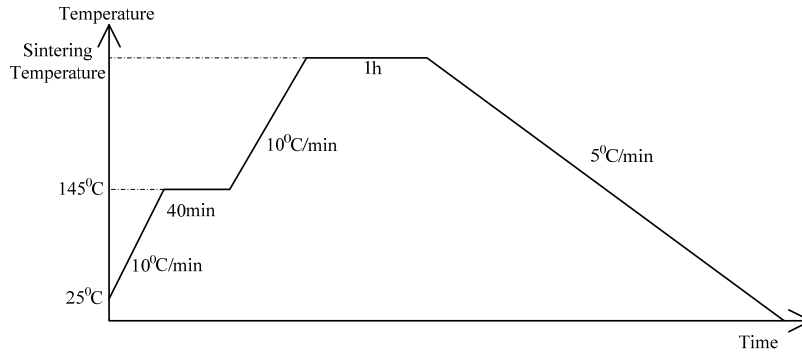


Figure 12. The sintering procedure used in our study.

Figure 13a shows an example of the built green part and the related sintered part (sintering temperature at 275°C). Figure 13b shows a set of gears that were sintered at different temperatures ranging from 200°C to 320°C . Compared to the fabricated green part that is also shown in Figure 13b, the dimensions of the sintered gears do not change much until $\sim 300^{\circ}\text{C}$. When the sintering temperature is set at 320°C , the green part shrinks significantly ($\sim 20\%$).

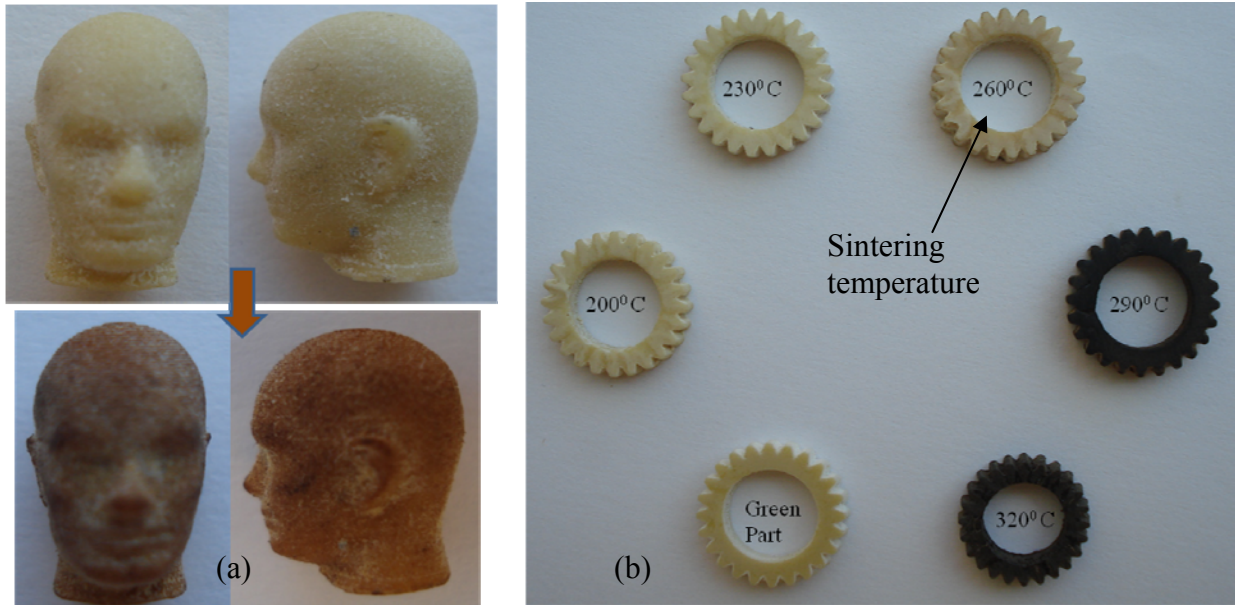


Figure 13. Parts before and after sintering.

As discussed in [14], sintering is a physically complex phenomenon, which results in numerous structural changes mass and significant improvement of its mechanical properties. The sintering

mechanism includes both surface and bulk transports. The initial stage of sintering mainly depends on surface diffusion. During the stage, there is little shrinkage. In contrast, the intermediate and final stages of sintering primarily depend on mass transport. A series of processes including interparticle bonding, neck growth, pore channel closure, pore rounding, and pore shrinkage will happen during the stages.

The test results as shown in Figure 13b illustrate that:

- (1) When the sintering temperature is $\leq 290^{\circ}\text{C}$, surface diffusion dominates the sintering of PEEK composite. The sintered parts are dimensionally accurate;
- (2) When the sintering temperature is $>300^{\circ}\text{C}$, mass transport exists in the sintering process of PEEK composite. Accordingly, the sintered part will shrink significantly.

Since large shrinkages are undesirable, the sintering temperatures in our material property study are set from 200°C to 290°C .

5. Material Property of Sintered Parts

5.1 Tensile test

We conducted tensile tests on the sintered parts. The tensile testing system we used is a 5KN Deben Micro Tensile module that is shown in Figure 14. Tensile bars with standard shapes and dimensions that are required by the testing machine were built. A sample test bar is shown in Figure 15a. A microscope combined with high resolution CCD was used to capture the shape changes of the tensile bar during the test. Figure 15 shows some example images of a tensile bar before and after the tensile test.

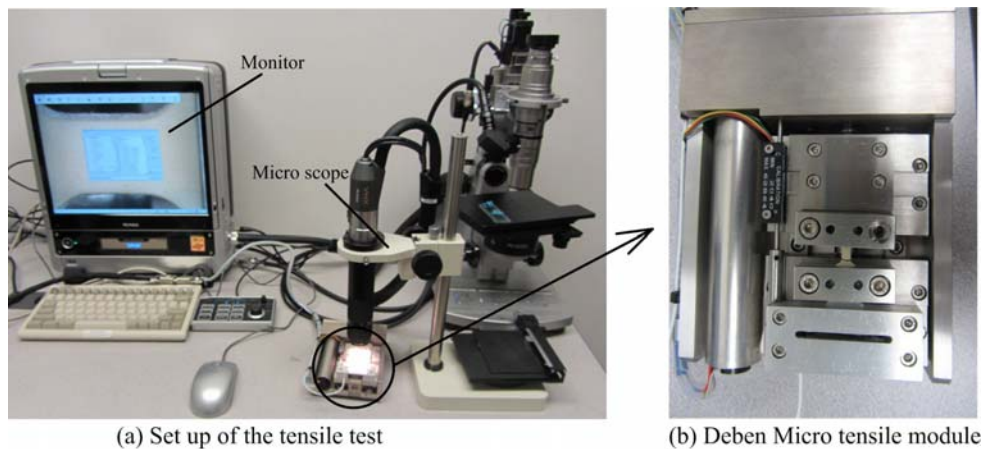


Figure 14. The setup for the tensile test.

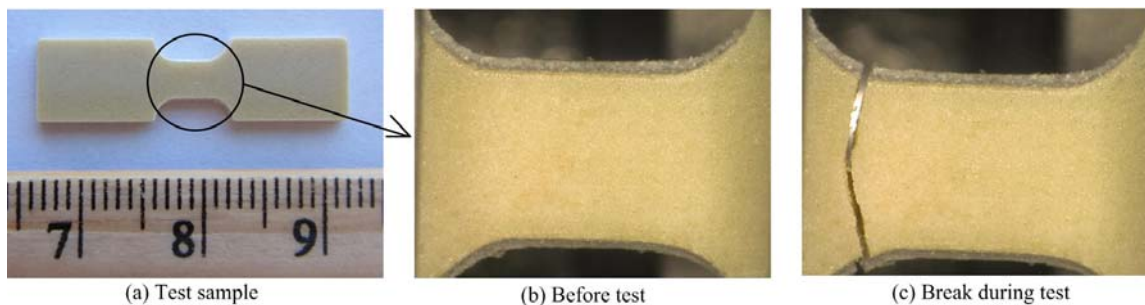


Figure 15. The shape and size of a tensile bar and captured images in the test.

The strain-stress curves generated from the tensile tests are shown in Figure 16. The Young's Modulus values of the related parts are shown in Table 1. It can be observed that the PEEK composite after sintering becomes stronger yet more brittle than the green part.

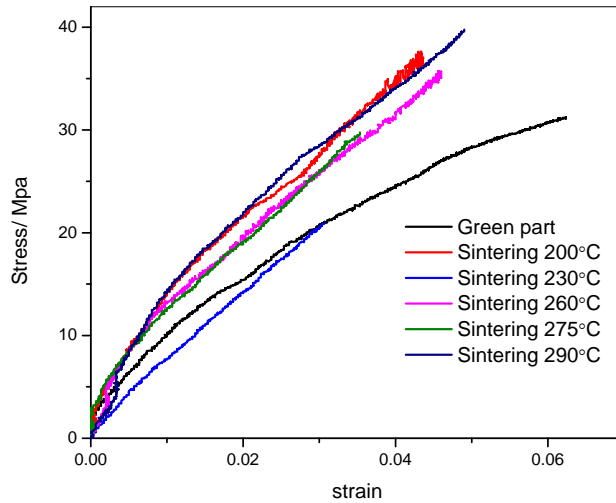


Figure 16. Stress-strain curves of the green part and the sintered parts.

Table 1. Young's Modulus values of the tested parts.

Sample type	Young's Modulus (MPa)
Green part without sintering	503
Sintering temperature 200 °C	822
Sintering temperature 230 °C	655
Sintering temperature 260 °C	716
Sintering temperature 275 °C	808
Sintering temperature 290 °C	776

5.2 Hardness test

Hardness tests on the sintered parts were conducted using a ROCKWELL hardness tester as shown in Figure 17. The scale of the hardness testing results is HRF. The testing results are shown in Table 2. Based on the results, we can see that the hardness of the built PEEK composite is affected by the sintering temperature. In addition, the sintered parts are harder than the green part. They are also harder than the part that is built in photocurable resin. In addition, the hardness of the sintered parts generally increases for a higher sintering temperature within our study range.



Figure 17. Wilson Rockwell hardness tester.

Table 2. Hardness values of the tested parts.

Sample Type	Hardness (HRF)
Pure resin part	29.5
Pure PEEK part	49.0
Green part without sintering	13.5
Sintering temperature 200 °C	52.5
Sintering temperature 230 °C	54.5
Sintering temperature 260 °C	57.0
Sintering temperature 275 °C	59.0
Sintering temperature 290 °C	61.0

5.3 Scanning electron microscope images

A Hitachi field emission scanning electron microscope (SEM) was used in capturing the micro-scale images of both the green and sintered parts. Figure 18 shows a comparison of the captured SEM images. It can be observed that the boundary of PEEK particles is obvious in the green part; however, it is difficult to distinguish the PEEK particles in the sintered sample (sintering temperature at 260°C for 1 hour). This verifies that the initial stage of sintering based on surface diffusion happens during the heat treatment process. The surface diffusion can be between neighboring PEEK particles and between PEEK particles and photocurable polymers.

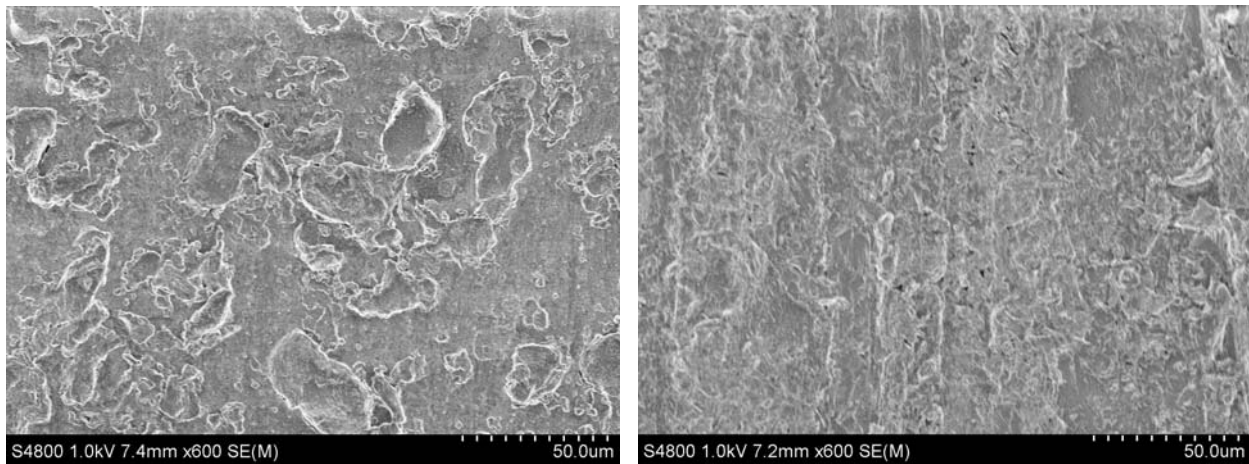


Figure 18. SEM images: (left) a green part; (right) a sintered part at 260°C.

6. Conclusion and Future Work

We investigated an alternative PEEK fabrication approach based on the mask-projection-based Stereolithography process. The developed additive manufacturing process includes slurry preparation, green part fabrication, and sintering. It is found that it is hard to generate mixed slurry with more than 37% of PEEK powders in the mixture without using additional chemical solutions. Hence the developed fabrication process will only be suitable for fabricating components of PEEK composite instead of pure PEEK. Three different recoating strategies have been developed for PEEK slurry with high viscosity values. The developed approaches can also be used in fabricating other types of powder-resin mixed slurry. We demonstrated that the sintering process can improve the strength and hardness of the built green parts. In addition, the sintered PEEK composite parts can have better material properties than those made in photocurable polymers without any PEEK particles.

The MIP-SL process can fabricate components with complex shapes. The process is also fast with a rather low cost. Although the use of MIP-SL in fabricating PEEK composite has been demonstrated in

our study, more efforts are required in each step to enable the process to build components with better material properties.

Acknowledgements

We acknowledge the support of ALM LLC., who provided us PEEK powders for the investigation. We also acknowledge Prof. Behrokh Khoshnevis and Prof. Steven Nutt at USC for their help on sintering and mechanical property testing, respectively.

References

- [1] Shekar, R. I., Kotresh, T. M., Rao, P. M. D., and Kumar, K.. (2009). Properties of high modulus PEEK yarns for aerospace applications. *Journal of Applied Polymer Science*, 112(4), 2497-2510. doi: 10.1002/app.29765.
- [2] Fu, H., Liao, B., Qi, F., Sun, B., Liu, A., and Ren, D. (2008). The application of PEEK in stainless steel fiber and carbon fiber reinforced composites. *Composites Part B*, 39(4), 585-591. doi: 10.1016/j.compositesb.2007.09.003.
- [3] Yu, S., Hariram, K. P., Kumar, R., Cheang, P., & Aik, K. K. (2005). In vitro apatite formation and its growth kinetics on hydroxyapatite/polyetheretherketone biocomposites. *Biomaterials*, 26(15), 2343-2352. doi: 10.1016/j.biomaterials.2004.07.028.
- [4] Li, Kai, Che Yan Yeung, Kelvin Wai, Kwok Yeung and Sie Chin Tjong (2012). Sintered Hydroxyapatite/Polyetheretherketone Nanocomposites: Mechanical Behavior and Biocompatibility, *Advanced Engineering Materials*, 2012, 14, No. 4.
- [5] Hope Molinaro. (2007). Carbon fiber-reinforced PEEK. *Plastics Engineering*, 63(4), 55.
- [6] Corni, I., Neumann, N., Novak, S., König, K., Veronesi, P., and Chen, Q. (2009). Electrophoretic deposition of PEEK-nano alumina composite coatings on stainless steel. *Surface and Coatings Technology*, 203(10), 1349-1359. doi: 10.1016/j.surfcoat.2008.11.005.
- [7] V. Balaji, A. N. Tiwari, R. K. Goyal (2009), Fabrication and Properties of High Performance PEEK/Si3N4 Nanocomposites. *Journal of Applied Polymer Science*, Vol. 119, 311–318.
- [8] Tan, K. H., Chua, C. K., Leong, K. F., Cheah, C. M., Cheang, P., Abu Bakar, M. S., and Cha, S. W. (2003). Scaffold development using selective laser sintering of polyetheretherketone–hydroxyapatite biocomposite blends. *Biomaterials*, 24(18), 3115-3123. doi: 10.1016/S0142-9612(03)00131-5.
- [9] Dietmar Drummer, Dominik Rietzel, Florian Kuhnlein (2010). Development of a characterization approach for the sintering behavior of new thermoplastics for selective laser sintering. *Physics Procedia*, vol. 5, 533–542.
- [10] Jing-Yi Zheng, Robert M. Pasternack, & Nada N. Boustany. (2009). Optical scatter imaging with a digital micromirror device. *Optics Express*, 17(22), 20401-20414.
- [11] Feather, G. A., & Monk, D. W. (2004). Digital micromirror device for projection display. 2407(1) doi: 10.1117/12.205883.
- [12] Chi Zhou, Yong Chen, Zhigang Yang, Behrokh Khoshnevis (2011). Development of Multi-material Mask-Image-Projection-based Stereolithography Process for the Fabrication of Digital Materials. *Proceedings of Solid Freeform Fabrication Symposium*, pp. 65-80, Austin, Texas, August 8~10, 2011.
- [13] Hamid Chabok, Chi Zhou, Yong Chen, Arash Eskandarinzhad, Qifa Zhou, and Kirk Shung (2012) Ultrasound Transducer Array Fabrication Based on Additive Manufacturing of Piezocomposites. *Proceedings of the ASME/ISCIE International Symposium on Flexible Automation (ISFA)*, St. Louis, Missouri, June 18-20, 2012.
- [14] German, R.M. (1994), *Powder metallurgy science*, 2nd ed., Metal Powder Industries Federation, Princeton.